

316 57

HIGH-FREQUENCY TECHNIQUES FOR RCS PREDICTION OF PLATE GEOMETRIES

Semiannual Progress Report

Constantine A. Balanis and Lesley A. Polka

February 1, 1991 - July 31, 1991

Department of Electrical Engineering
Telecommunications Research Center
Arizona State University
Tempe, Arizona 85287-7206

Grant No. NAG-1-562
National Aeronautics and Space Administration
Langley Research Center
Hampton, VA 23665

HIGH-FREQUENCY TECHNIQUES FOR RCS PREDICTION
OF PLATE GEOMETRIES Semiannual Progress
Report, 1 Feb. - 31 Jul. 1991 (Arizona
State Univ.) 3P D

CSCL 20N

N91-27440

Unclas

H1/32 0031637

HIGH-FREQUENCY TECHNIQUES FOR RCS PREDICTION OF PLATE GEOMETRIES

Semiannual Progress Report

Constantine A. Balanis and Lesley A. Polka

February 1, 1991 - July 31, 1991

Department of Electrical Engineering
Telecommunications Research Center
Arizona State University
Tempe, Arizona 85287-7206

Grant No. NAG-1-562
National Aeronautics and Space Administration
Langley Research Center
Hampton, VA 23665

ABSTRACT

This report discusses radar cross section (RCS) prediction of several rectangular plate geometries using high-frequency techniques such as the Uniform Theory of Diffraction (UTD) for perfectly conducting and impedance wedges and the Method of Equivalent Currents (MEC). Previous reports have presented detailed solutions to the principal-plane scattering by a perfectly conducting and a coated rectangular plate and nonprincipal-plane scattering by a perfectly conducting plate. This report briefly reviews these solutions and presents a modified model for the coated plate.

Theoretical and experimental data is presented for the perfectly conducting geometries. Agreement between theory and experiment is very good near and at normal incidence. In regions near and at grazing incidence, the disagreement between the data varies according to diffraction distances and angles involved. It is these areas of disagreement which are of extreme interest as an explanation for the disagreement will yield invaluable insight into scattering mechanisms which have not yet been identified as major contributors near and at grazing incidence. This report identifies and examines areas of disagreement between theory and experiment in an attempt to better understand and predict near-grazing incidence, grazing incidence, and nonprincipal-plane diffractions.

I. INTRODUCTION

Previous reports have presented models for principal-plane scattering from perfectly-conducting and coated rectangular plates and for nonprincipal-plane scattering from a perfectly conducting rectangular plate [1]-[5]. The models for principal-plane scattering were based upon a traditional application of the Geometrical Theory of Diffraction (GTD)/Uniform Theory of Diffraction (UTD) method developed by Keller [6] and Kouyoumjian and Pathak [7]. For the case involving a coating on a perfectly conducting plate, the impedance wedge diffraction coefficients developed by Tiberio *et al.* [8] and Griesser and Balanis [9] were used. The coating was modeled using the impedance boundary condition. The model for nonprincipal-plane scattering was based upon several versions of the Method of Equivalent Currents (MEC) developed by Michaeli [10]-[14]. Currents to account for corner scattering were added using a model for quarter-plane scattering developed by Hansen [15] using numerical techniques.

These geometries are basic but very important because their simplicity allows the isolation and study of several important scattering mechanisms. The chief scattering mechanism involved in principal-plane scattering from a rectangular plate is the diffraction between parallel wedges. Also of importance in this geometry is the effect of the two edges parallel to the plane of incidence. For a

rectangular plate with a coating, the effect of the coating is also of importance. There are several important mechanisms involved in the nonprincipal-plane scattering from a rectangular plate. Among these are first-order scattering from each of the four edges, higher-order scattering as a result of interactions among the edges, and corner scattering from each of the four corners.

The high-frequency models reported previously are very accurate at and near normal incidence. Depending upon the exact scattering configuration, these models begin to fail to varying degrees. For principal-plane scattering from the perfectly conducting plate, results are in almost exact agreement with experimental data for soft polarization. For the hard polarization case, the theoretical results compare well with the experimental data except within a few degrees of grazing and directly at grazing incidence. The amount of disagreement between theory and experiment increases as the distance between main diffraction points becomes electrically small. A measure of the validity of the GTD/UTD model with respect to plate width and incidence angle is of interest as is an explanation of the disagreement between experiment and theory. This report looks more closely at the problems involved in predicting the scattering near and at grazing incidence using high-frequency models.

The coated plate model reported previously contained only first-order terms. The plane-wave incidence and far-field scattering

conditions necessary for radar cross section (RCS) prediction were approximated by assuming cylindrical-wave incidence and diffraction at very large distances. These approximations were necessary because the diffraction coefficients [8], [9] used were for cylindrical-wave incidence and diffraction. This report presents modified coefficients for plane-wave incidence, far-field observation. A new model for first-order scattering from the coated plate is presented. To correct for caustics at normal incidence, a physical optics (PO) model is used near and at normal incidence. The PO model is combined with the UTD model to provide a comprehensive first-order model.

The case of nonprincipal-plane scattering from a rectangular plate is more complicated than the principal-plane case. Discrepancies between theory and experiment are greater and exist in regions at grazing incidence and up to 45° away from grazing incidence in some instances. A number of reasons exist for these discrepancies. This report details these explanations, some interesting experimental trends, and some possible model improvements.

In most cases, the moment method (MM) is more accurate than high-frequency methods in the problem areas near grazing incidence. With the advent of faster computers with larger memories, this technique is not as inconvenient to use as it once was. Low-frequency techniques such as the MM, however, do not provide the insight into the scattering mechanisms that high-frequency techniques such as the

UTD and the MEC afford. In addition, as the dimensions of a scatterer become electrically large, low-frequency models become quite computationally cumbersome while high-frequency techniques become increasingly more accurate without sacrificing computational speed.

II. THEORY AND RESULTS

A. PRINCIPAL-PLANE SCATTERING FROM A PERFECTLY CONDUCTING, RECTANGULAR PLATE

The GTD/UTD model for principal-plane scattering from a perfectly conducting rectangular plate is covered in detail in [1]; therefore, the details of the model will not be repeated here. Briefly, the model is based on a straightforward application of the GTD and of the UTD coefficients for diffraction between two points. The model is, thus, a two-dimensional model for an infinite strip which is truncated to form an equivalent rectangular plate. Ross's truncation approximation [16] is used to convert the two-dimensional scattering width of the infinite strip into the three-dimensional RCS of the corresponding rectangular plate of length L :

$$\sigma_{3-D} \cong \frac{2L^2}{\lambda} \sigma_{2-D} \quad (1)$$

The GTD coefficients are used for first-order diffractions and the UTD coefficients for higher-order terms. For the soft polarization, higher-order diffraction terms do not exist; however, slope diffraction terms [17] are included in the soft polarization

model as these terms contribute slightly near and at grazing incidence. The hard polarization model includes higher-order diffractions between the edges. In theory, an infinite number of terms could be included; however, in practice, terms higher than fourth-order contribute negligibly. The results shown in this report include first-, second-, third-, and fourth-order terms only.

The plate geometry is shown in Fig. 1. The planes of incidence and diffraction are the x-y plane. Experimental and theoretical results are shown in Figs. 2-5. The smaller plate considered has a width of $\lambda/2$ and a length of 6λ . The larger plate has a width of 2λ and a length of 6λ . The thickness of the plates is 0.00271λ ; however, in order to experimentally simulate an infinitely thin scatterer, the edges in the plane of incidence were filed to a point. Monostatic RCS measurements were performed in Arizona State University's (ASU's) anechoic chamber at a frequency of 10 GHz.

The agreement between theory and experiment is very good for the soft polarization case, even down to a width of $\lambda/2$, which is approaching the lower bound of validity for a UTD solution. The results for the hard polarization case are, again, excellent near and at normal incidence. As grazing incidence is approached, the discrepancy between theory and experiment increases. The amount and extent of the disagreement decreases as the diffraction distance becomes larger. The agreement is very good up to approximately 5° of

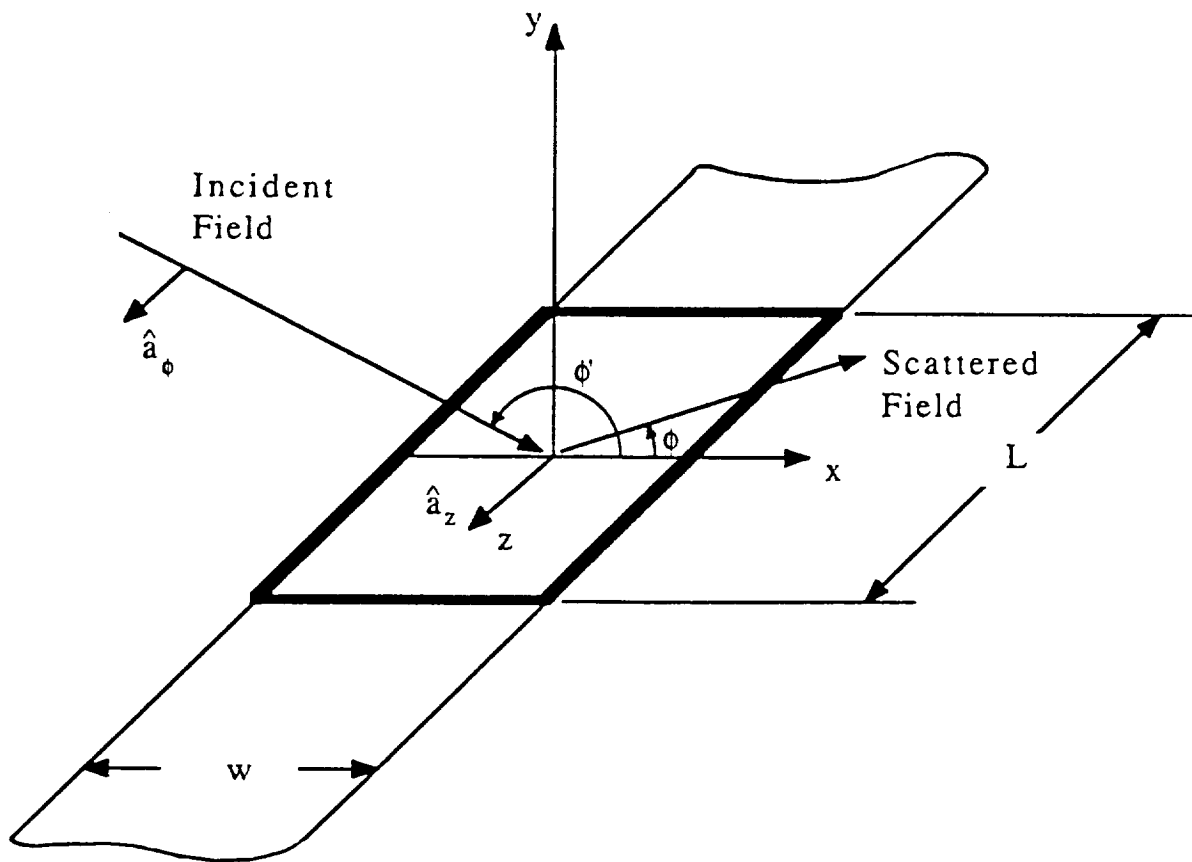


Fig. 1. Strip/plate geometry.

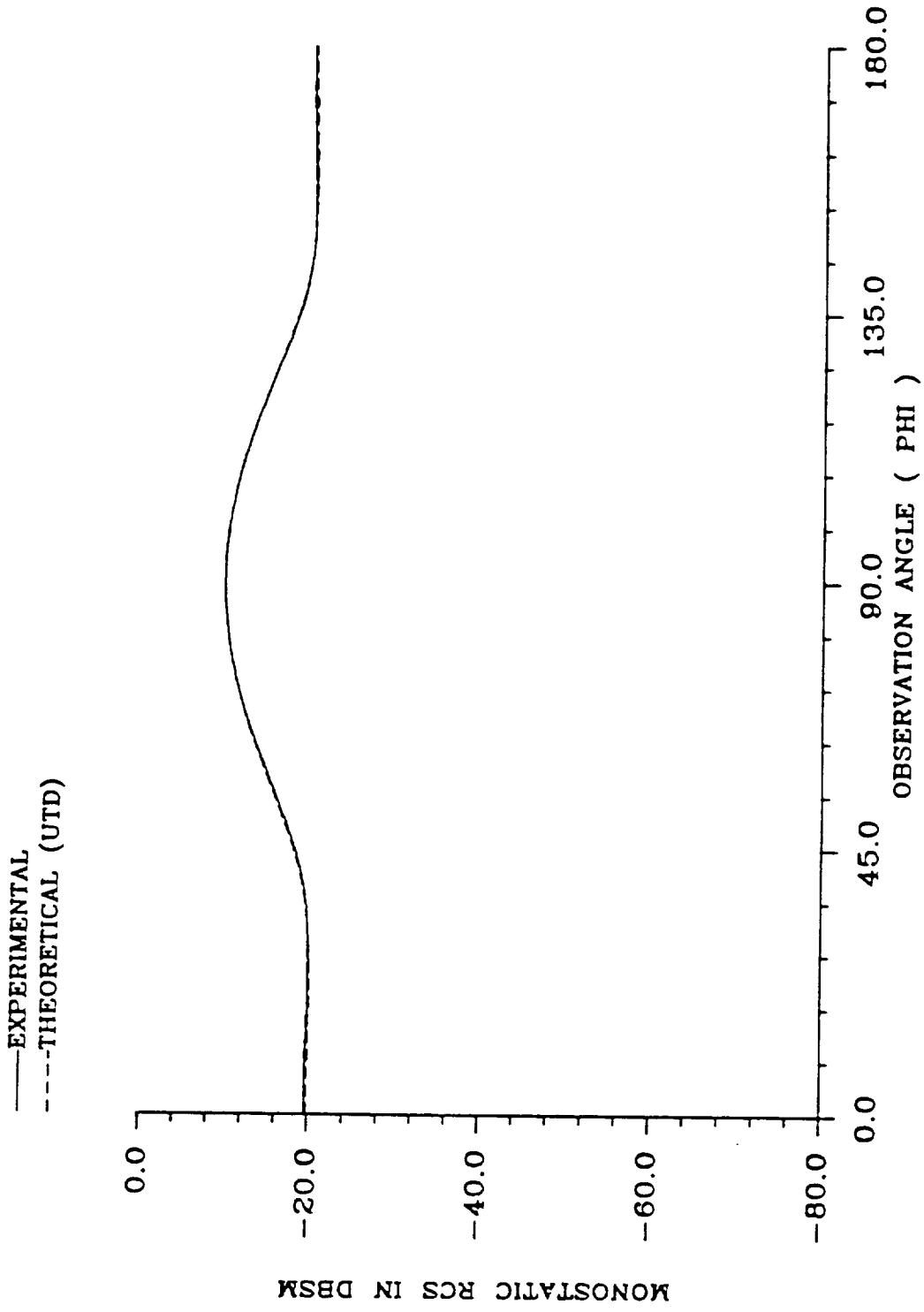


Fig. 2. Monostatic RCS of a rectangular plate ($w=\lambda/2$, $L=6\lambda$, principal plane, soft polarization, $f=10$ GHz).

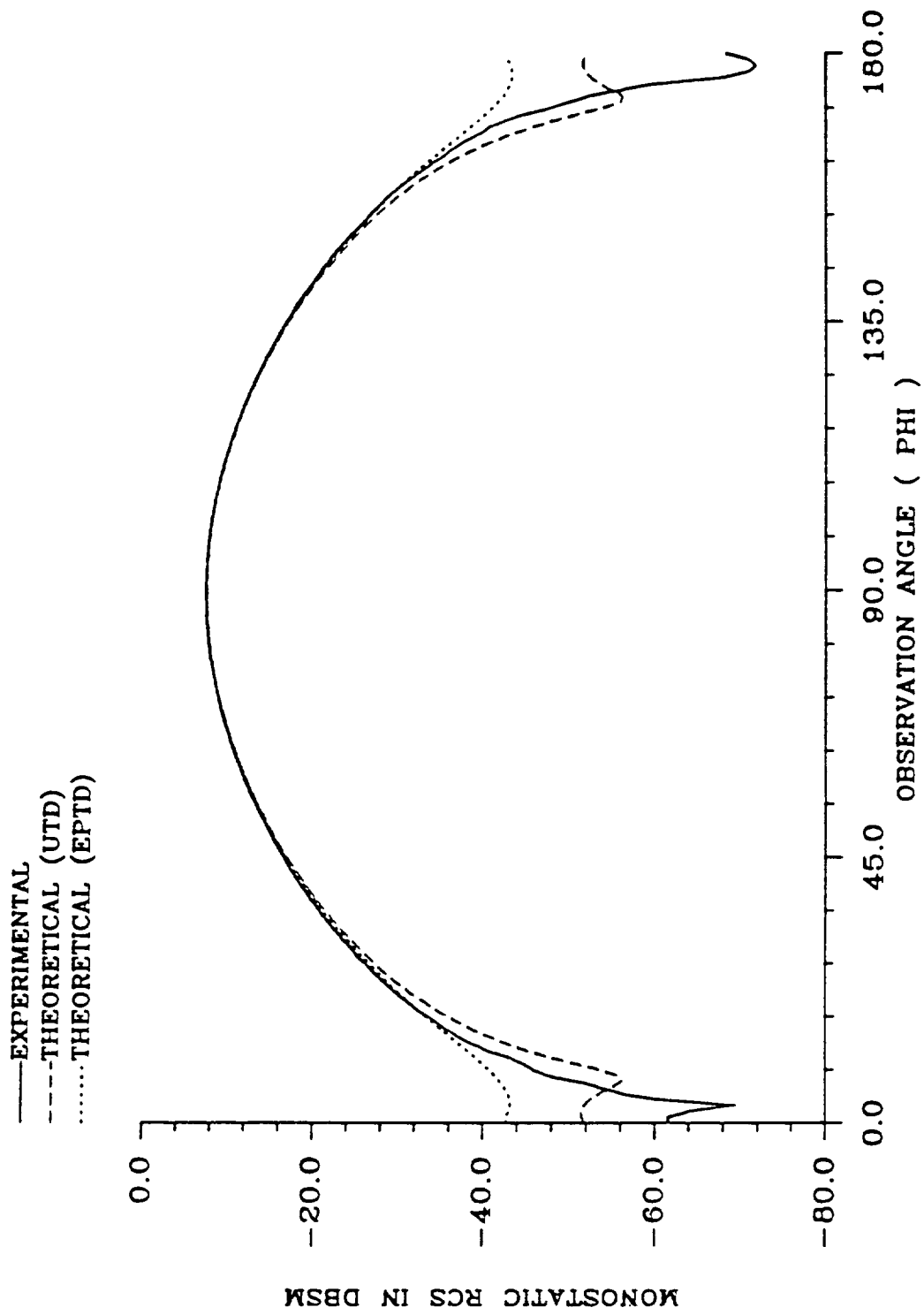


Fig. 3. Monostatic RCS of a rectangular plate ($w=\lambda/2$, $L=6\lambda$, principal plane, hard polarization, $f=10$ GHz).

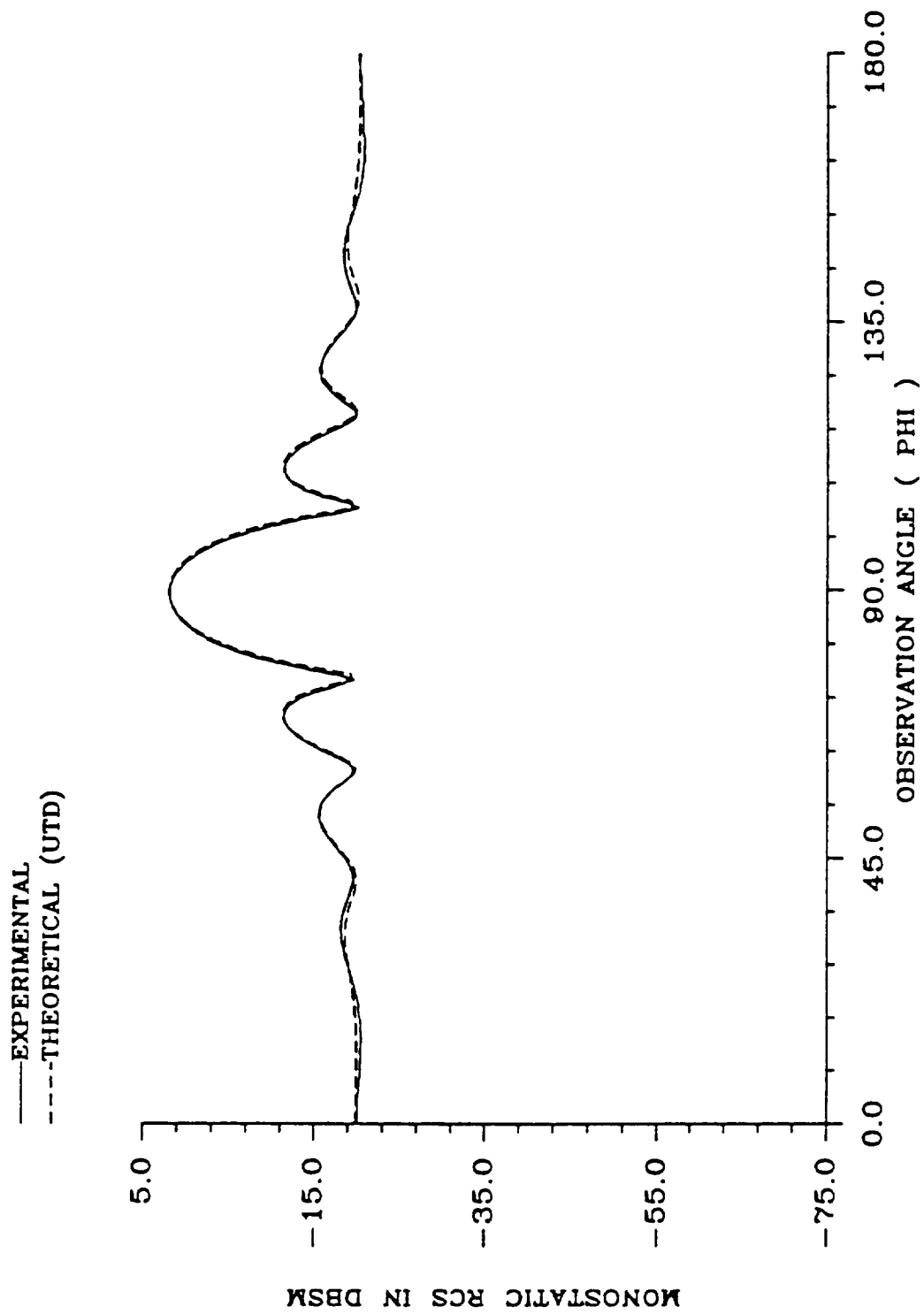


Fig. 4. Monostatic RCS of a rectangular plate ($w=2\lambda$, $L=6\lambda$, principal plane, soft polarization, $f=10$ GHz).

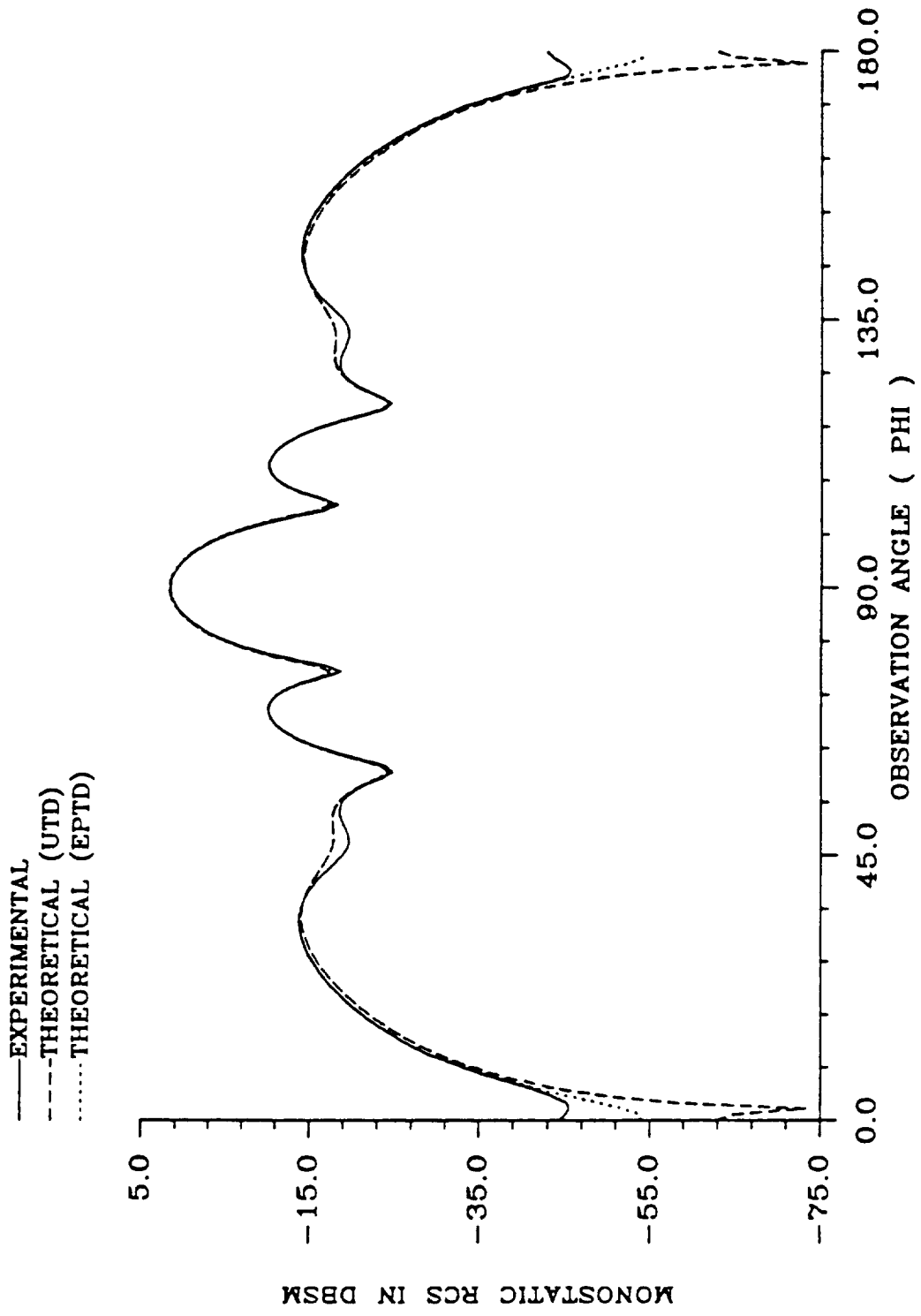


Fig. 5. Monostatic RCS of a rectangular plate ($w=2\lambda$, $L=6\lambda$, principal plane, hard polarization, $f=10$ GHz).

grazing incidence for the 2λ width plate; however, disagreement is evident in the $\lambda/2$ width case within 20° of grazing.

There are three possible sources of error in the UTD model. The first and most theoretically disturbing error involves using a straightforward, more or less blind, application of the UTD in calculating the first-order field incident on the second edge of diffraction. The UTD is not valid in overlapping transition regions, which exist in the forward scattering region for grazing and near-grazing incidence, due to the non-ray-optical nature of the field in that region [18].

Two extended theories have been developed to deal with this specific case of second-order diffraction due to a non-ray-optical incident field resulting from diffraction within overlapping transition regions [19], [20]. Tiberio et al. [19] developed a method based upon a spectral extension of the UTD. Michaeli's method [20] is based upon an extension of the Physical Theory of Diffraction (PTD) and involves an asymptotic evaluation of the radiation integral. Results from Michaeli's model for strip scattering are included in Figs. 3 and 5, the hard polarization cases, and are labeled as EPTD, or Extended Physical Theory of Diffraction, results. The soft polarization case does not involve higher-order diffractions; therefore, the invalidity of the UTD in overlapping transition regions is not a source of error in the soft polarization results.

The results in Figs. 3 and 5 illustrate that the error in the UTD is a small source of error near and at grazing incidence but is not the only, or even most significant, source of error. The EPTD does result in a marked improvement over the UTD in the case involving the smaller diffraction distance of $\lambda/2$ in Fig. 3. The EPTD results disagree with the experimental data only within 10° of grazing whereas the UTD disagrees as far as 20° from grazing. For the larger diffraction distance of 2λ , the difference between the EPTD and the UTD results is less obvious. The region of disagreement with experiment extends from grazing to approximately 5° from grazing for both models. In the region of disagreement, the EPTD results are much closer to the experimental results than the UTD results are; however, the amount of disagreement is still large enough to warrant inspection of other sources of error.

Two other possible sources of error are truncation error and thickness error. The truncation error, which results from using Eq. (1) to convert from the two-dimensional scattering width of an infinite strip to the three-dimensional RCS of a rectangular plate, arises because the effects of the two edges parallel to the plane of incidence are neglected. The thickness error results from not accounting for the finite thickness of the plate. Both the UTD and the EPTD models use the truncation approximation of Eq. (1) and assume an infinitely thin scatterer.

These errors cannot be corrected by an obvious application of a high-frequency technique. In order to investigate the magnitude of the effects of the two edges parallel to the plane of incidence and of the thickness, the results of several different MM models are compared with the experimental data for the hard polarization case for both the $\lambda/2$ -width and the 2λ -width plate in Figs. 6 and 7. The first MM model determines the two-dimensional scattering width of an infinite strip with a finite thickness. Eq. (1) is then used to convert to the three-dimensional RCS of the finite strip. This model, which is designated as MM(2-D), includes, therefore, only truncation error.

The second MM model, MM(3-D, $t=0$), is a three-dimensional model which assumes an infinitely thin plate, or a thickness of 0. This model, therefore, includes only thickness error. The final MM model, MM(3-D), is a three-dimensional model with a finite thickness so that no truncation or thickness errors are included.

The results in Figs. 6 and 7 indicate that the truncation error is much more significant than the thickness error. For both the $\lambda/2$ -width plate and the 2λ -width plate, the differences between the MM(2-D), which includes truncation error only, and the MM(3-D), which contains neither truncation nor thickness error, models are significant near and at grazing incidence. The differences between the MM(3-D, $t=0$), which includes thickness error only, and the MM(3-D)

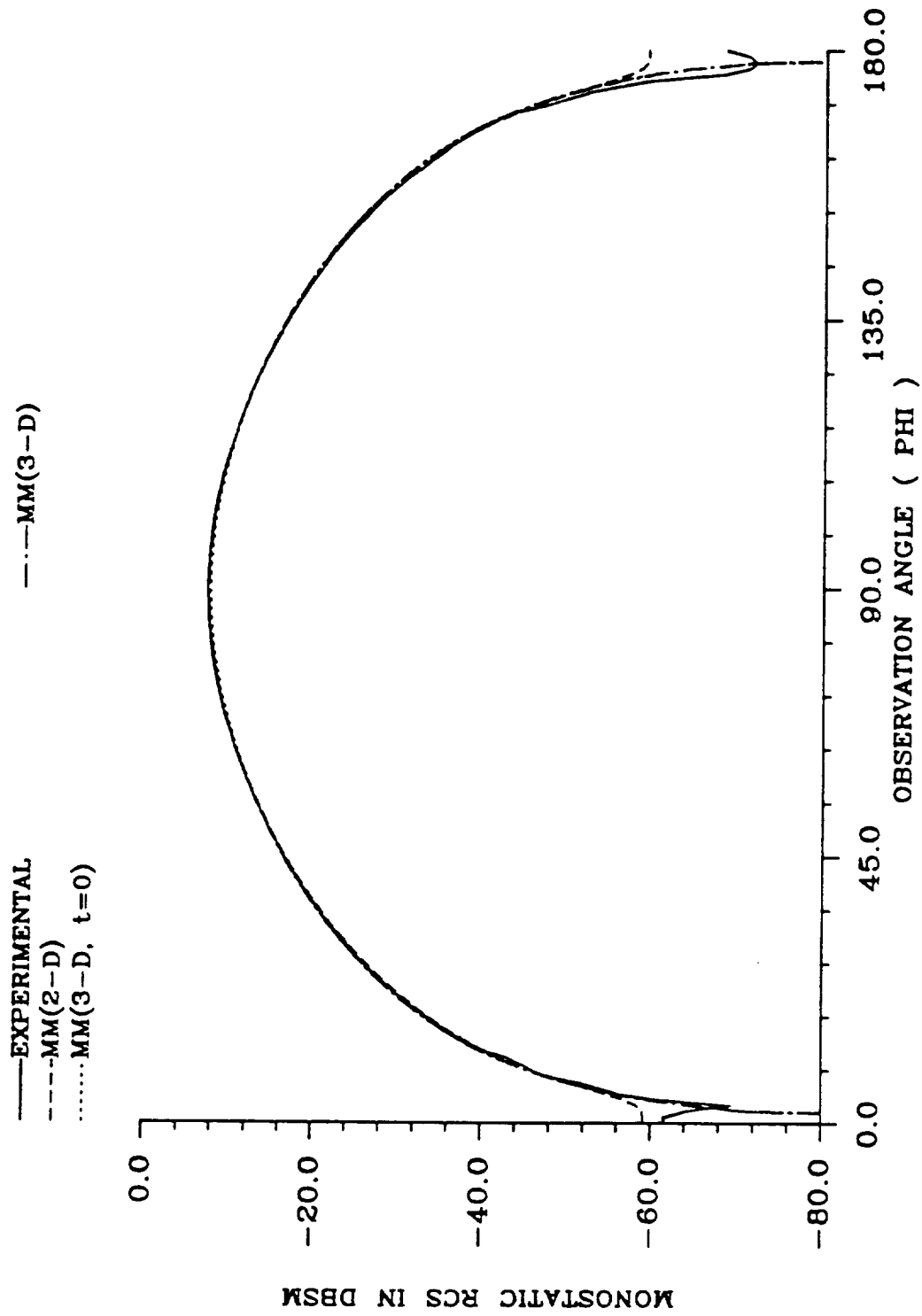


Fig. 6. Monostatic RCS of a rectangular plate ($w=\lambda/2$, $L=6\lambda$, Principal plane, hard polarization, $f=10$ GHz).

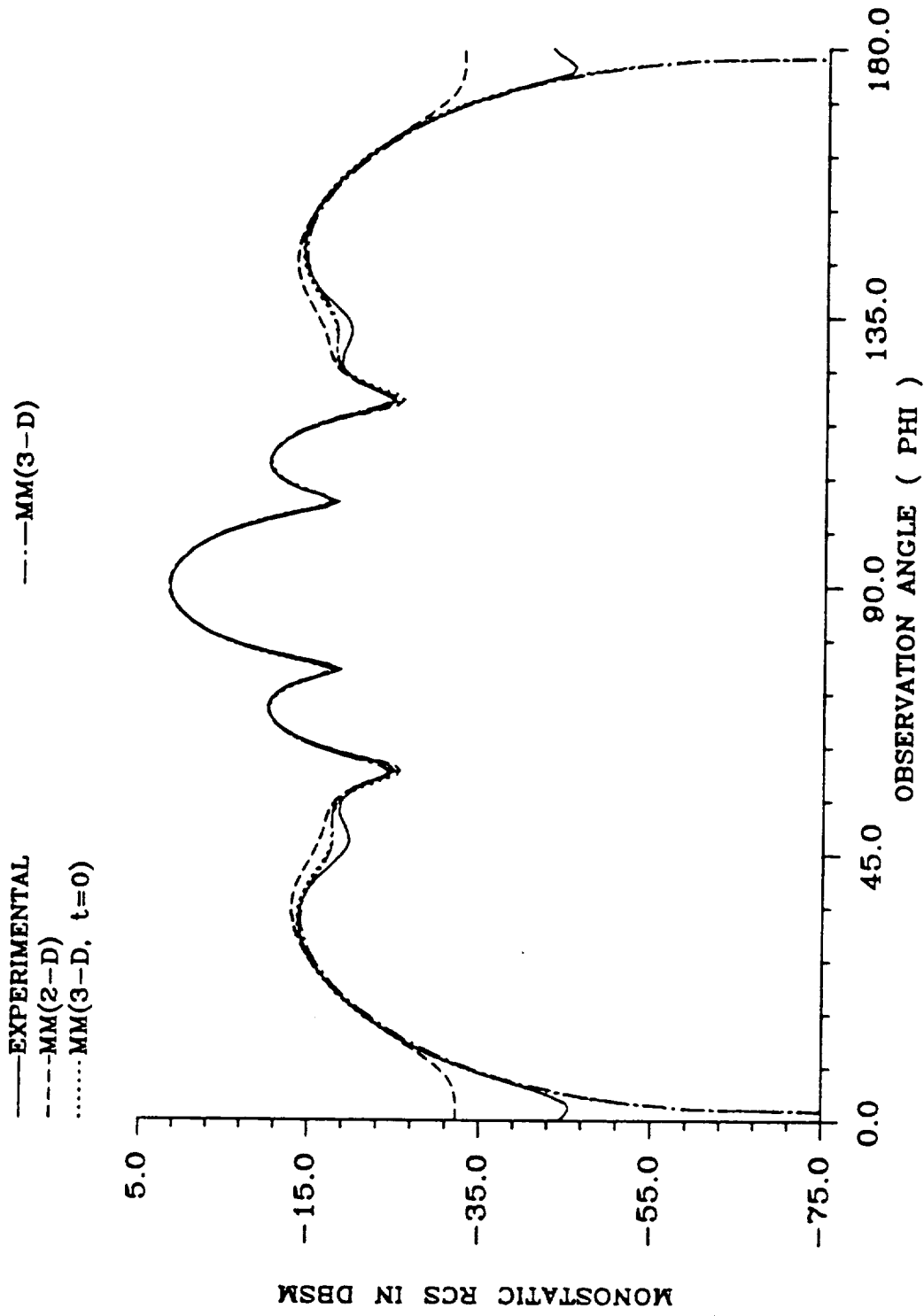


Fig. 7. Monostatic RCS of a rectangular plate ($w=2\lambda$, $L=6\lambda$, principal plane, hard polarization, $f=10$ GHz).

model are so minimal that the graphs of the results from the two models are indistinguishable in Figs. 6 and 7.

A final observation concerning the results in Figs. 6 and 7 involves the angular ranges over which the truncation and the thickness errors are important. Significant differences between the experimental results and the results of MM(3-D, $t=0$) extend from grazing incidence to approximately 5° from grazing. This range of discrepancy due to thickness error is the same for both the $\lambda/2$ and the 2λ plate. The angular range of discrepancy between experiment and theory for the MM(2-D) model, however, increases with increasing plate width. For the $\lambda/2$ plate the angular range of errors extends from grazing to approximately 5° from grazing. For the 2λ plate the angular range of error extends much further from grazing to approximately 12° from grazing. Truncation errors, thus, appear to increase in significance with increasing plate width.

It is curious to note that differences between theory and experiment still exist near and at grazing incidence for the MM(3-D) model although both truncation and thickness effects are accounted for in this model. This indicates that there may be another scattering mechanism that is not yet identified that is significant near and at grazing incidence.

B. PRINCIPAL-PLANE SCATTERING FROM A COATED, RECTANGULAR PLATE

Previous reports [1], [2] have presented models for first-order diffraction from the coated plate geometry of Fig. 8. This model was based upon the UTD diffraction coefficients developed by Tiberio et al. [8] and Griesser and Balanis [9], which are for cylindrical-wave incidence and diffraction. To incorporate these coefficients into an RCS model, plane-wave incidence and far-field observation were approximated using large source and observation distances. These approximations, though valid, involved other approximations for the monostatic scattering configuration that were not aesthetically pleasing. In an attempt to remedy the problems involved, a new model based upon a far-field diffraction coefficient similar to Keller's GTD coefficient for perfectly conducting structures [6] has been formulated.

The truncation approximation of Eq. (1) is used to convert the two-dimensional scattering width of an infinite, coated strip to the three-dimensional RCS of the coated, rectangular plate. The expression for the scattering width is:

$$\sigma_{2-D} = 2\pi \left\{ D_1 e^{-j(kw/2)(\cos\phi' + \cos\phi)} + D_2 e^{j(kw/2)(\cos\phi' + \cos\phi)} \right\} \quad (2)$$

where

$$D_1 = \text{DCFF}(\text{polarization}, \phi', \phi, 2, \theta_o, \theta_2)$$

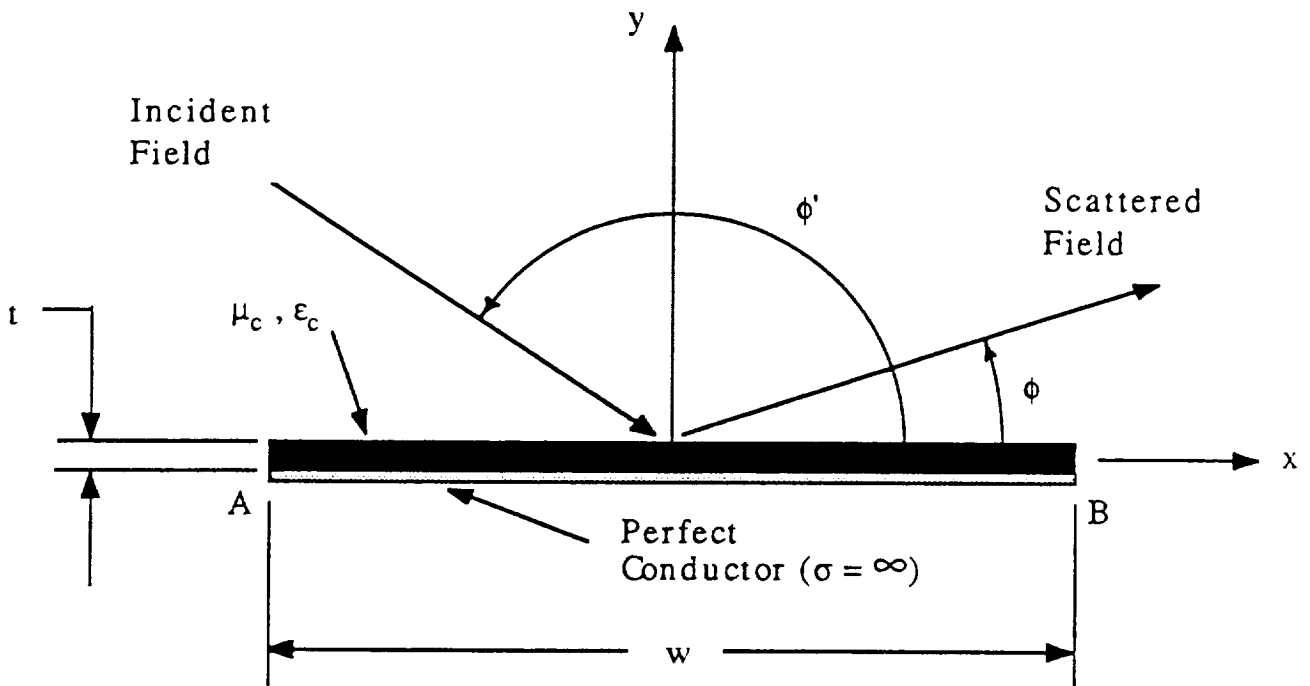


Fig. 8. Coated strip/plate geometry.

$$D_2 = \text{DCFF}(\text{polarization}, \begin{matrix} \pi-\phi' & (0^\circ \leq \phi' \leq 180^\circ) & \pi-\phi & (0^\circ \leq \phi \leq 180^\circ) \\ 3\pi-\phi' & (180^\circ \leq \phi' \leq 360^\circ) & 3\pi-\phi & (180^\circ \leq \phi \leq 360^\circ) \end{matrix}, 2, \theta_o, \theta_n)$$

and $\text{DCFF}(\text{polarization}, \phi', \phi, n, \theta_o, \theta_n)$ is the diffraction coefficient for the impedance wedge developed in [8] and [9] with all the Fresnel transition functions set to 1. This eliminates all distance parameters and is, effectively, a far-field solution. ϕ' and ϕ are the incidence and diffraction angles. n is the wedge parameter, which is 2 for the half planes used to approximate the plate geometry. θ_o and θ_n are the Brewster angles associated with the equivalent impedance of the coating. These have been explained in detail in previous reports [1], [2].

To avoid caustics at and near normal incidence, a PO formulation is used at these angles. A standard PO approach [17] is adopted with the reflection coefficient for the coated side formulated in terms of the equivalent impedance of the coated plate. The reflection coefficients are:

Soft Polarization

$$\Gamma_{\text{soft}} = \frac{\eta_{\text{eq}} \sin\phi_i - \sin\phi_t}{\eta_{\text{eq}} \sin\phi_i + \sin\phi_t} \quad (3)$$

Hard Polarization

$$\Gamma_{\text{hard}} = \frac{\sin\phi_i - \eta_{\text{eq}} \sin\phi_t}{\sin\phi_i + \eta_{\text{eq}} \sin\phi_t} \quad (4)$$

where

$$\eta_{eq} = j \sqrt{\frac{\mu_c}{\epsilon_c}} \tan(2\pi\sqrt{\mu_c\epsilon_c} t \sin\phi_t) \quad (5)$$

where

t = coating thickness in free-space wavelengths

μ_c = relative permeability of the coating

ϵ_c = relative permittivity of the coating

and

$$\sin\phi_t = \sqrt{1 - \frac{1}{\mu_c\epsilon_c} \cos^2\phi_i}$$

For the perfectly conducting side of the plate, the PO expressions for the RCS are:

$$\sigma_{soft} = \frac{(kwL)^2}{\pi} \sin^2\phi' \left\{ \frac{\sin((kw/2)(\cos\phi' + \cos\phi))}{(kw/2)(\cos\phi' + \cos\phi)} \right\}^2 \quad (6)$$

$$\sigma_{hard} = \frac{(kwL)^2}{\pi} \sin^2\phi \left\{ \frac{\sin((kw/2)(\cos\phi' + \cos\phi))}{(kw/2)(\cos\phi' + \cos\phi)} \right\}^2 \quad (7)$$

For the coated side of the plate, the PO expressions are:

$$\sigma_{soft} = |\Gamma_{soft}|^2 \frac{(kwL)^2}{\pi} \sin^2\phi' \left\{ \frac{\sin((kw/2)(\cos\phi' + \cos\phi))}{(kw/2)(\cos\phi' + \cos\phi)} \right\}^2 \quad (8)$$

$$\sigma_{hard} = |\Gamma_{hard}|^2 \frac{(kwL)^2}{\pi} \sin^2\phi \left\{ \frac{\sin((kw/2)(\cos\phi' + \cos\phi))}{(kw/2)(\cos\phi' + \cos\phi)} \right\}^2 \quad (9)$$

The UTD and PO models are combined to provide a comprehensive model for first-order diffraction from the coated plate. Results from this model will be presented in the next reporting period.

Higher-order diffraction terms and surface-wave terms will also be incorporated to complete the model.

C. NONPRINCIPAL-PLANE SCATTERING FROM A RECTANGULAR PLATE

Details for the MEC models that have been used to predict the RCS in nonprincipal planes for the rectangular plate of Fig. 9 are included in previous reports and will not be repeated here. The most consistently successful model has been the model using the GTD-based equivalent currents of [10] combined with Hansen's currents [15] to account for corner scattering.

Briefly, the model consists of currents placed along each of the four edges to account for first-order diffraction from the edges. Corner currents are placed along edges 1 and 3 to account for scattering due to corner A. Hansen's corner current model has only been developed for an angular range of $0^\circ \leq \phi' \leq 90^\circ$, so scattering due to the other three corners cannot be included using this model. Results from this model are compared with experimental data and MM data in Figs. 10-13.

The plate considered is 17.18 cm on a side. Measurements were performed at 10 GHz. The best agreement between theory and experiment was obtained for the 30° -rotated plate, soft polarization case shown in Fig. 10. The region of largest disagreement between theory and experiment occurs within 15° of grazing incidence. The results near

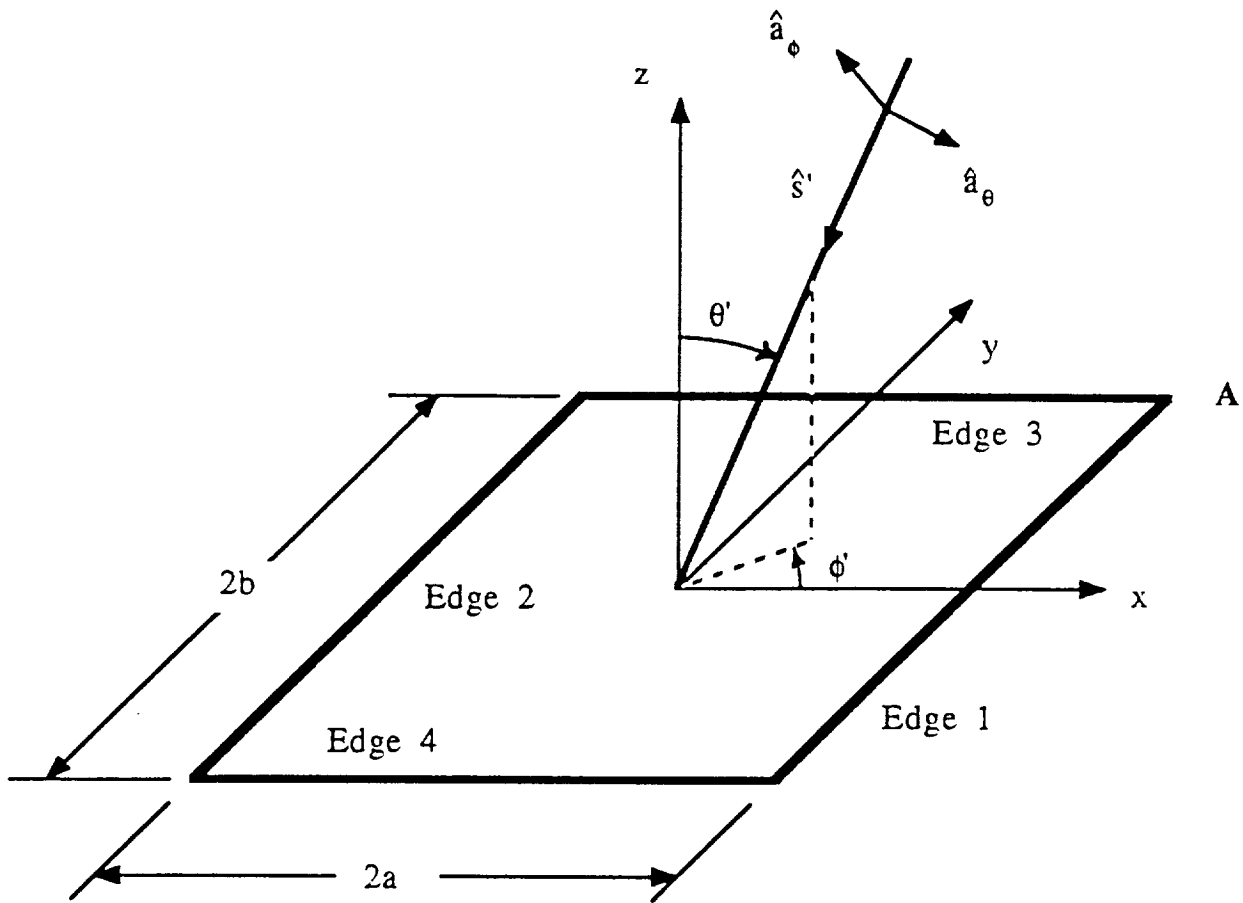


Fig. 9. Rectangular plate geometry.

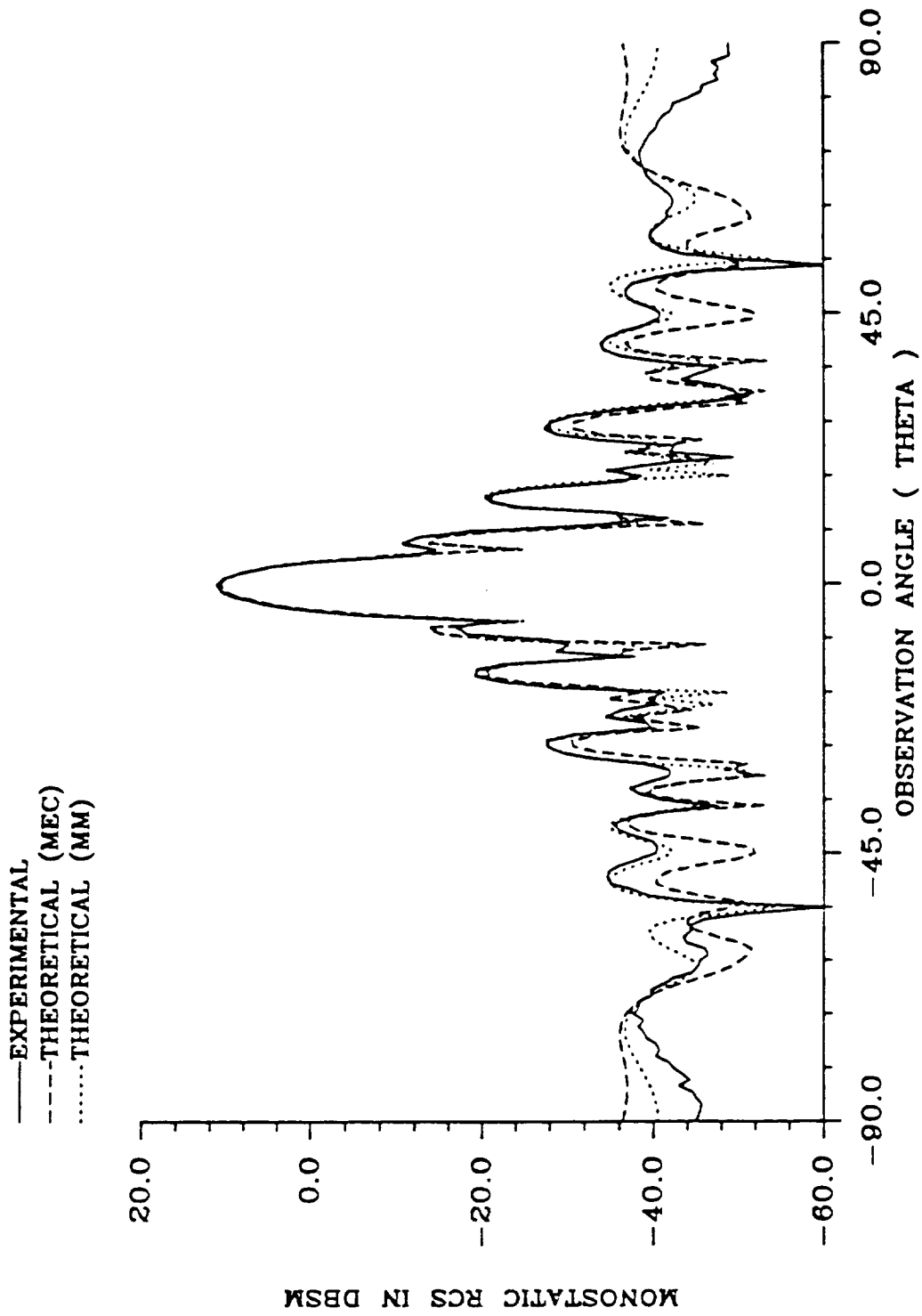


Fig. 10. Monostatic RCS of a square plate (soft polarization, $2a=2b=17.18$ cm, $f=10$ GHz, $\phi'=30^\circ$).

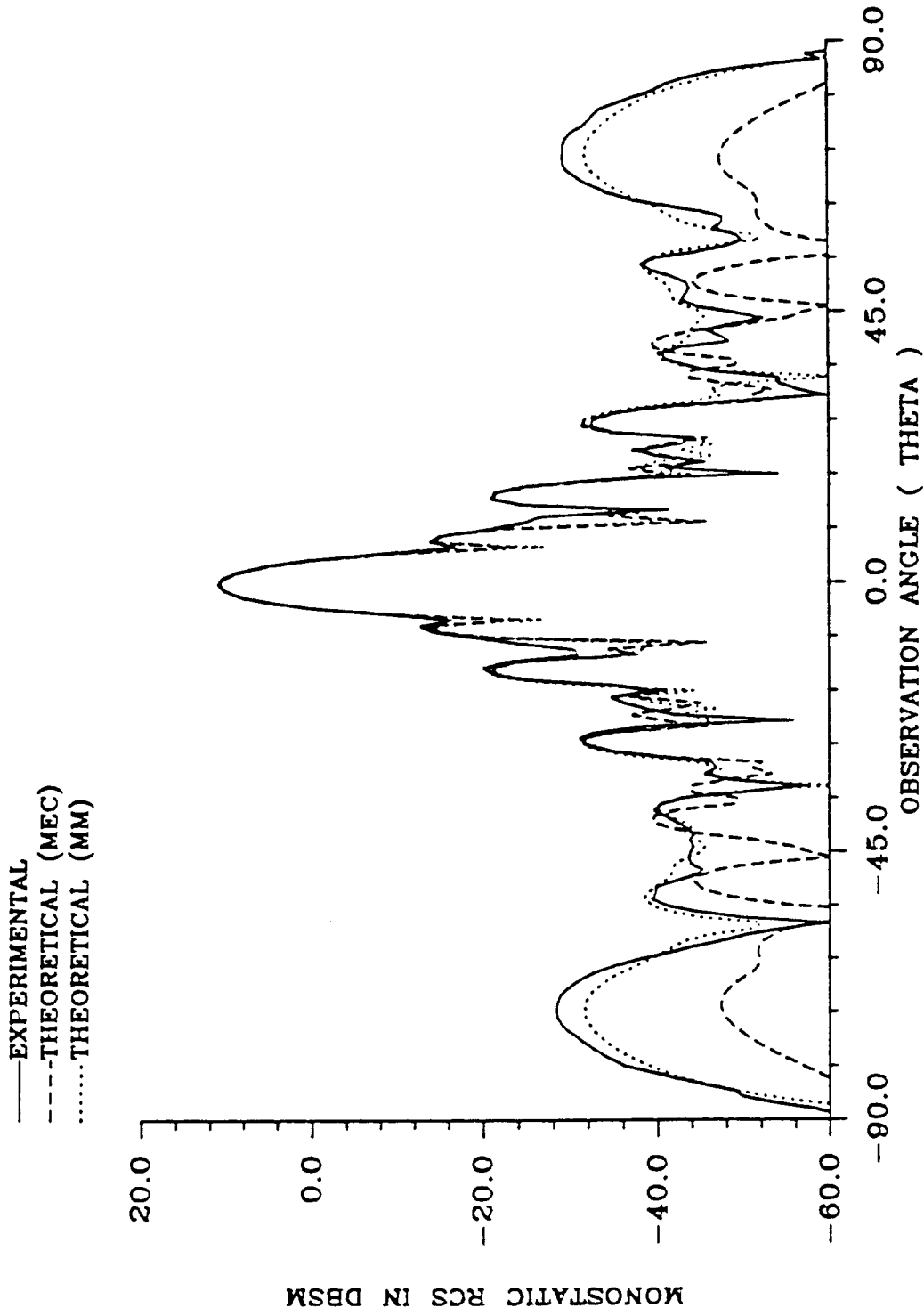


Fig. 11. Monostatic RCS of a square plate (hard polarization,
 $2a=2b=17.18$ cm, $f=10$ GHz, $\phi'=30^\circ$).

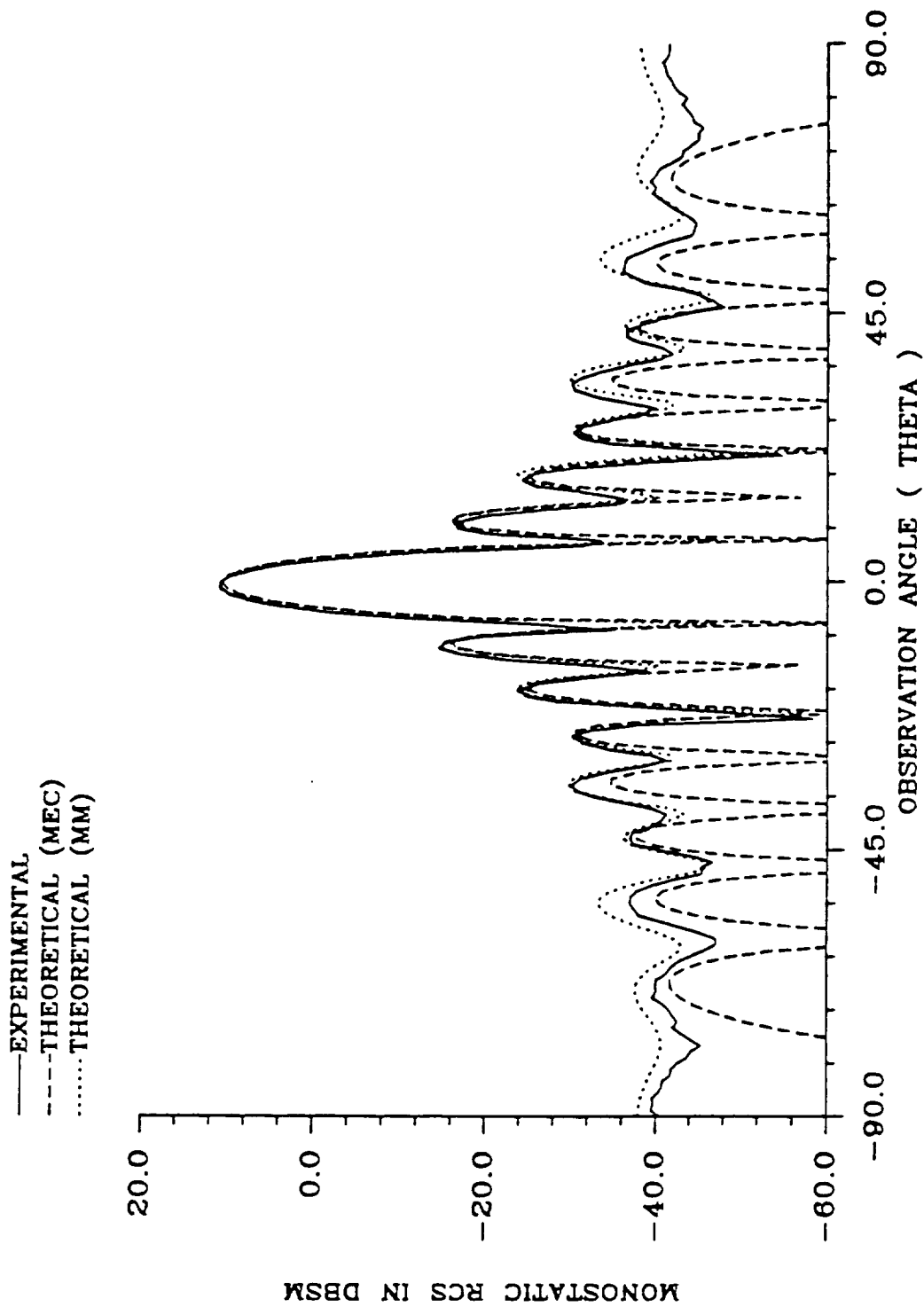


Fig. 12. Monostatic RCS of a square plate (soft polarization,
 $2a=2b=17.18$ cm, $f=10$ GHz, $\phi'=45^\circ$).

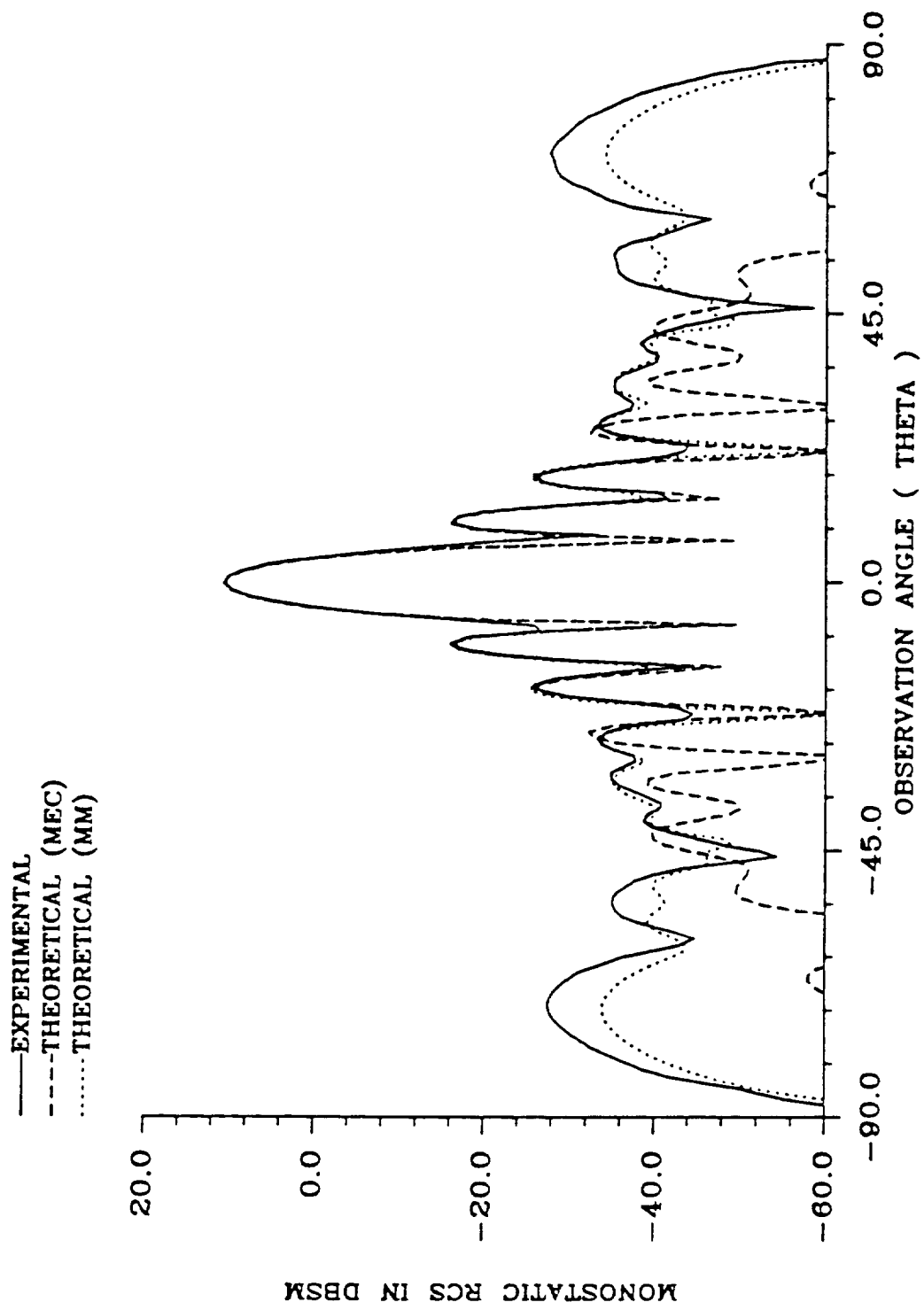


Fig. 13. Monostatic RCS of a square plate (hard polarization, $2a=2b=17.18$ cm, $f=10$ GHz, $\phi'=45^\circ$).

grazing incidence are greatly improved over previous models [4], which included edge diffraction only, by the addition of the corner currents which account for scattering from corner A. This is not the case for the other rotation angles and polarizations shown in the remaining figures. In these cases, the magnitude of the corner current field is so small that it does not noticeably affect the results.

The disagreement between theory and experiment for the hard polarization case at a rotation angle of 30° , shown in Fig. 11, extends over a much larger range than for the soft polarization case. There are large disagreements in the range from 30° away from grazing up to grazing. The most noticeable flaw in the theoretical model is that it fails to predict a very major lobe that occurs near grazing incidence with a peak at approximately 18° from grazing.

The trends observed for a rotation angle of 45° in Figs. 12 and 13 are similar to those for the 30° rotation angle. The soft polarization results are in good agreement until approximately 10° away from grazing. There is a much larger discrepancy between the theoretical and experimental results for the hard polarization case. Major differences appear up to 40° from grazing and continue up to grazing incidence. As for the 30° -rotated plate at hard polarization, the major flaw in the theoretical model is that it fails to predict a major lobe that peaks at approximately 18° from grazing incidence.

Two possible sources of the differences that occur between the theoretical and the experimental data are the failure of the theoretical model to include corner diffraction terms for all four corners and to include second-order scattering terms that take into account double diffractions between opposite and adjacent sides. The importance of including a valid corner diffraction model is obvious. Especially for the 45° -rotated plate of Figs. 12 and 13, which involves incidence and observation in the plane that cuts through two corners, it seems intuitively evident that corner diffraction mechanisms are important and that a corner diffraction term will greatly improve the results near and at grazing incidence.

The significance and effects of second-order scattering mechanisms are less intuitively obvious; however, the comparisons of Figs. 14 and 15 lead to some interesting conclusions about the major, as yet unpredicted, lobes that occur near grazing incidence in the hard polarization case and about second-order scattering. Fig. 13 once again presents the experimental data for the hard polarization case for both the 30° - and 45° -rotated plates. As expected, the lobing structure, away from normal incidence, of the two sets of measurements is completely different; however, near grazing incidence, the lobe that appears is nearly identical in both cases. This indicates that this lobe is very insensitive to plate rotation.

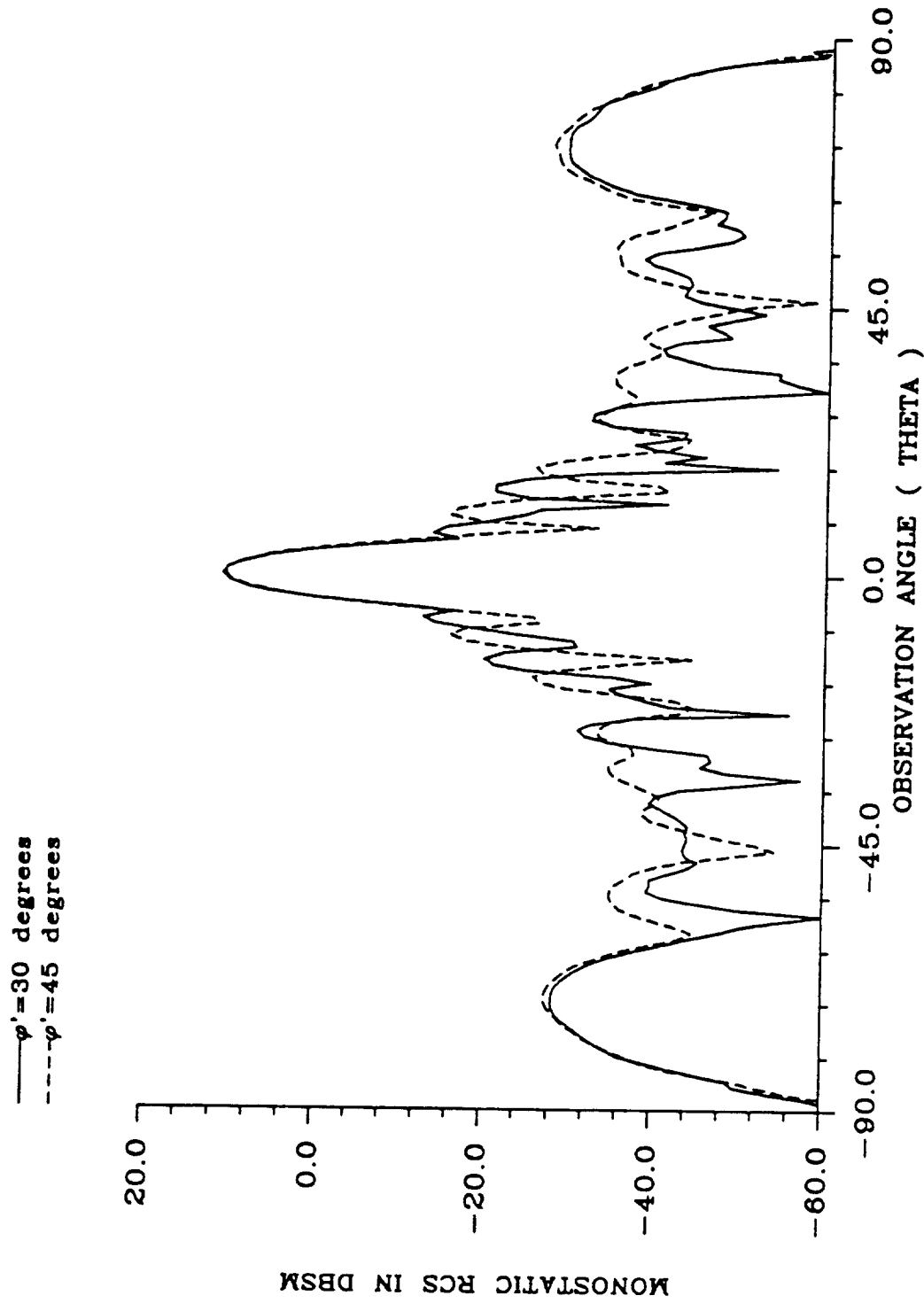


Fig. 14. Monostatic RCS of a square plate (hard polarization, $2a=2b=17.18$ cm, $f=10$ GHz).

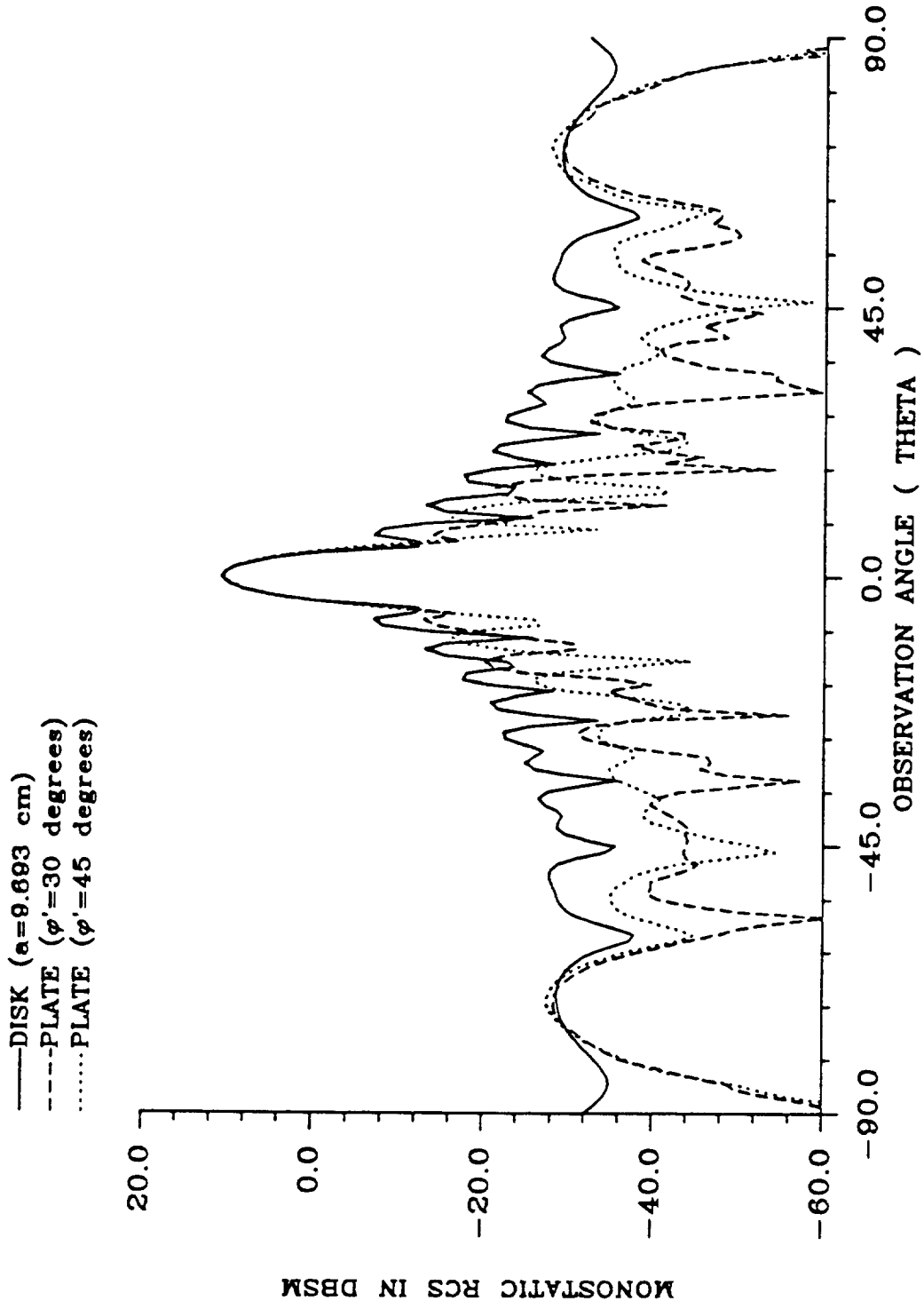


Fig. 15. Monostatic RCS of a disk (UTD model) vs. monostatic RCS of a square plate (experimental data) (disk: radius=9.693 cm, plate: $2a=2b=17.18$ cm; hard polarization, $f=10$ GHz).

Fig. 15 provides more information which may assist in predicting this lobe. In this graph, the RCS of a disk of the same physical area as the rectangular plate and for the hard polarization case is superimposed on the data from Fig. 14. The disk RCS data is from the GTD/UTD disk model formulated by Marsland et al. [21], which yields very good agreement with experimental results. The disk and rectangular-plate RCS patterns differ significantly away from normal incidence, as expected; however, the major lobe near grazing appears at the same location and has the same magnitude for both targets. An analysis of the scattering terms included in the disk model indicates that the only terms responsible for the accurate prediction of the lobe are the terms for second-order diffraction between main scattering points in the plane of incidence. This is important information for modeling the same phenomenon for the rectangular plate.

III. FUTURE WORK

A detailed examination of several high-frequency models for basic plate geometries has provided important information for revising these models to better predict phenomena that occur near and at grazing incidence and in nonprincipal planes. Future work will concentrate on revisions to the present models and experimental work to validate

theoretical results and to further isolate specific scattering mechanisms that occur for these plate geometries.

Although the present model for principal-plane scattering from a perfectly conducting, rectangular plate provides very good agreement with experimental results for plates as small as $\lambda/2$ in width, there remain discrepancies near and at grazing incidence which should be accounted for. The investigations of this reporting period indicate that truncation effects that arise in converting the scattering width of a two-dimensional, infinite strip to the RCS of a three-dimensional rectangular plate are significant in the regions of disagreement between theory and experiment and that the significance of truncation effects increases with increasing plate width. Future work will involve accounting for the scattering from the two edges of the plate parallel to the plane of incidence so that truncation effects will be avoided. Two models that will be considered are the application of the UTD coefficients and of equivalent currents.

The UTD model for first-order scattering from the coated plate has been modified so that fewer approximations are involved. Future work will involve obtaining numerical results from this model and further enhancement of the model to include higher-order diffraction terms and surface-wave terms.

The present investigation yields crucial information for improving the model for nonprincipal-plane scattering from the

perfectly conducting, rectangular plate. Specifically, the major, as yet unpredicted, lobe that occurs near grazing incidence in the hard polarization case appears to be relatively insensitive to rotation angle of the plate and appears to be due to second-order diffraction. Future work will involve modeling the second-order diffractions that account for this lobe and modeling corner diffraction. Experimental work will also be undertaken to provide more data for comparisons at other rotation angles and to isolate various scattering mechanisms.

The ultimate goal of this research is to isolate, explain, and predict fundamental scattering mechanisms that are not, yet, fully understood. Among these are grazing incidence scattering in both principal and nonprincipal planes, corner scattering, and scattering from thinly coated structures. An understanding of these mechanisms will enable the development of more complete high-frequency models for more complicated structures.

IV. REFERENCES

- [1] C. A. Balanis and L. A. Polka, "High-frequency techniques for RCS prediction of plate geometries," Semiannual Report, Grant No. NAG-1-562, National Aeronautics and Space Administration, Langley Research Center, Hampton, VA, Jan. 31, 1991.
- [2] C. A. Balanis, L. A. Polka, K. Liu, "Scattering from coated structures and antenna pattern control using impedance surfaces," Semiannual Report, Grant No. NAG-1-562, National Aeronautics and Space Administration, Langley Research Center, Hampton, VA, Jul. 31, 1990.

- [3] ———, "Nonprincipal-plane scattering from rectangular plates and pattern control of horn antennas," Semiannual Report, Grant No. NAG-1-562, National Aeronautics and Space Administration, Langley Research Center, Hampton, VA, Jan. 31, 1990.
- [4] ———, "Nonprincipal-plane scattering from flat plates — second-order and corner diffraction and pattern control of horn antennas," Semiannual Report, Grant No. NAG-1-562, National Aeronautics and Space Administration, Langley Research Center, Hampton, VA, Jul. 31, 1989.
- [5] ———, "Nonprincipal plane scattering of flat plates and pattern control of horn antennas," Semiannual Report, Grant No. NAG-1-562, National Aeronautics and Space Administration, Langley Research Center, Hampton, VA, Jan. 31, 1989.
- [6] J. B. Keller, "Geometrical theory of diffraction," *J. Opt. Soc. Amer.*, vol. 52, pp. 116-130, Feb. 1962.
- [7] R. G. Kouyoumjian and P. H. Pathak, "A uniform geometrical theory of diffraction for an edge in a perfectly conducting surface," *Proc. IEEE*, vol. 62, pp. 1448-1461, Nov. 1974.
- [8] R. Tiberio, G. Pelosi, and G. Manara, "A uniform GTD formulation for the diffraction by a wedge with impedance faces," *IEEE Trans. Antennas Propagat.*, vol. AP-33, pp. 867-873, Aug. 1985.
- [9] T. Griesser and C. A. Balanis, "Reflections, diffractions, and surface waves for an interior impedance wedge of arbitrary angle," *IEEE Trans. Antennas Propagat.*, vol. AP-37, pp. 927-935, July 1988.
- [10] A. Michaeli, "Equivalent edge currents for arbitrary aspects of observation," *IEEE Trans. Antennas Propagat.*, vol. AP-32, pp. 252-258, Mar. 1984.
- [11] ———, "Correction to 'Equivalent edge currents for arbitrary aspects of observation'," *IEEE Trans. Antennas Propagat.*, vol. AP-33, p. 227, Feb. 1985.
- [12] ———, "Elimination of infinities in equivalent edge currents, part I: fringe current components," *IEEE Trans. Antennas Propagat.*, vol. AP-34, pp. 912-918, July 1986.
- [13] ———, "Elimination of infinities in equivalent edge currents, part II: physical optics components," *IEEE Trans. Antennas Propagat.*, vol. AP-34, pp. 1034-1037, Aug. 1986.

- [14] —, "Equivalent currents for second-order diffraction by the edges of perfectly conducting polygonal surfaces," *IEEE Trans. Antennas Propagat.*, vol. AP-35, pp. 183-190, Feb. 1987.
- [15] T. B. Hansen, "An investigation of the currents due to right-angled corners of flat plates," Technical Report, Electromagnetics Institute, Technical University of Denmark, Jan. 1990.
- [16] R. A. Ross, "Radar cross section of rectangular flat plates as a function of aspect angle," *IEEE Antennas Propagat.*, vol. AP-14, pp. 329-335, May 1966.
- [17] C. A. Balanis, *Advanced Engineering Electromagnetics*. New York: John Wiley & Sons, 1989.
- [18] R. Tiberio and R. G. Kouyoumjian, "A uniform GTD solution for the diffraction by strips illuminated at grazing incidence," *Radio Science*, vol. 14, pp. 933-941, Nov.-Dec. 1979.
- [19] R. Tiberio, G. Manara, G. Pelosi, and R. G. Kouyoumjian, "High-frequency electromagnetic scattering of plane waves from double wedges," *IEEE Trans. Antennas Propagat.*, vol. AP-37, pp. 1172-1180, Sept. 1989.
- [20] A. Michaeli, "A uniform GTD solution for the far-field scattering by polygonal cylinders and strip," *IEEE Trans. Antennas Propagat.*, vol. AP-35, pp. 983-986.
- [21] D. P. Marsland, C. A. Balanis, and S. A. Brumley, "Higher order diffractions from a circular disk," *IEEE Trans. Antennas Propagat.*, vol. AP-35, pp. 1436-1444, Dec. 1987.